STRUCTURAL CHEMISTRY

ISSN 2053-2296

Crystal structures of three β-halolactic acids: hydrogen bonding resulting in differing Z′

Matthew N. Gordon, Yanyao Liu, Ibrahim H. Shafei, M. Kevin Brown and Sara E. Skrabalak*

Department of Chemistry, Indiana University Bloomington, 800 E. Kirkwood Ave., Bloomington, IN 47405, USA. *Correspondence e-mail: sskrabal@iu.edu

Received 22 January 2022
Accepted 14 March 2022

Edited by I. Oswald, University of Strathclyde, United Kingdom

Keywords: crystal structure; Z′; hydrogen bonding; halogen bonding; Hirshfeld surface; halolactic acid.

CCDC references: 2102491; 2102492; 2102493

Supporting information: this article has supporting information at journals.iucr.org/c

The crystal structures of three β-halolactic acids have been determined, namely, β-chlorolactic acid (systematic name: 3-chloro-2-hydroxypropanoic acid, $C_3H_5ClO_3$) (I), β-bromolactic acid (systematic name: 3-bromo-2-hydroxypropanoic acid, $C_3H_5BrO_3$) (II), and β-iodolactic acid (systematic name: 2-hydroxy-3-iodopropanoic acid, $C_3H_5IO_3$) (III). The number of molecules in the asymmetric unit of each crystal structure (Z′) was found to be two for I and II, and one for III, making I and II isostructural and III unique. The difference between the molecules in the asymmetric units of I and II is due to the direction of the hydrogen bond of the alcohol group to a neighboring molecule. Molecular packing shows that each structure has alternating layers of intermolecular hydrogen bonding and halogen–halogen interactions. Hirshfeld surfaces and two-dimensional fingerprint plots were analyzed to further explore the intermolecular interactions of these structures. In I and II, energy minimization is achieved by lowering of the symmetry to adopt two independent molecular conformations in the asymmetric unit.

1. Introduction

Lactic acid is a compound found throughout biology and used as a synthetic intermediate in the biochemical industry. It is an α-hydroxy acid, a carboxylic acid with a hydroxy group on the adjacent C atom. Both functionalities are highly hydrophilic; therefore, these molecules are used widely as cosmetic agents due to their ability to penetrate skin and relieve photo-damaged skin (Tang & Yang, 2018). Additionally, lactic acid can self-polymerize through condensation to form poly(lactic acid) chains useful as a biodegradable plastic (Inkinen *et al.*, 2011). Lastly, molecules of lactic acid can also be used as chelators for metal ions (Sayre *et al.*, 2010; Souaya *et al.*, 2014). Therefore, derivatives of lactic acid with added functionalities are advantageous.

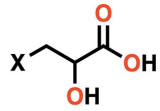

X = Cl (I), Br (II), or I (III)

Scheme 1

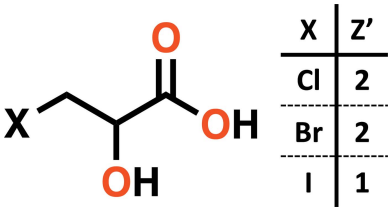

Alkyl halides are tremendously versatile compounds in the toolbox of the organic chemist. They are effective reagents in nucleophilic and radical alkylation, as well as in cross-coupling reactions. The identity of the halogen has a strong influence on the stability and reactivity of an alkyl halide given the differences in the size, polarizability, and electronegativity of the halogen. In crystal engineering, substitution of the halide has led to structural changes (Johnson *et al.*, 2012) and changes in magnetic properties (Kühne *et al.*, 2020). Deepening the

understanding of these structure–property relationships will benefit the chemical industry, from medicinal chemistry to natural product synthesis.

Herein, we report the crystal structures of three halide-substituted lactic acids, namely, β-chlorolactic acid (I), β-bromolactic acid (II), and β-iodolactic acid (III). With the halogen spatially separated from the α-hydroxy acid, these molecules can be used in alkylation reactions to add an α-hydroxy acid moiety to a substrate. Polymerization of these reagents may lead to other poly(lactic acid)-derived biodegradable plastics with properties that can be tuned based on halogen identity. The crystal structures of these three compounds have been analyzed, with the goal of identifying and understanding the crystallographic changes that occur with changes in halogen identity. The number of molecules in the asymmetric unit in each structure (Z') was found to vary.

The reason certain crystal structures have $Z' > 1$ is not fully understood (Steed & Steed, 2015). One explanation is that a structure with $Z' = 1$ may not be able to fulfill the optimum intermolecular interactions (*e.g.* hydrogen bonding), and so this 'packing frustration' is alleviated by adopting a higher Z'. Another rationale suggests that $Z' > 1$ crystals are kinetically trapped metastable phases caused by preassociated dimers/clusters under solution or nucleation conditions. While a single explanation is not agreed upon, a combination of multiple factors may determine which structures have $Z' > 1$.

$Z' > 1$ structures do have some common features that differ from those found in $Z' = 1$ structures. The presence of an alcohol –OH functional group is found in 22.0% of structures with $Z' = 2$, compared to 20.3% for $Z' = 1$ structures. A carboxylic acid functional group is found in 4.3% of $Z' = 2$ structures compared to 4.1% of $Z' = 1$ structures (Gavezzotti, 2008). The halolactic acids studied here contain both functional groups, increasing their likelihood of having $Z' > 1$. Angelo Gavezzotti wrote that 'each case (of $Z' = 2$) may be a story in itself'. Here we hope to tell one of those stories.

2. Experimental

2.1. Synthesis and crystallization

Analytical grade reagents were used as received without additional purification. The three compounds are chiral molecules and are produced in a way that gives a racemic mixture for crystallization. Both enantiomers appear in the structures by symmetry. Instrumental details are provided in *Appendix A* of the supporting information.

The synthesis of I was carried out according to a modified literature procedure (Baumruck *et al.*, 2018). To a 250 ml round-bottomed flask with a stirrer bar was added (±)-3-chloropropane-1,2-diol (11.05 g, 100 mmol), followed by the addition of 30 ml nitric acid (conc.). **(CAUTION: handling large amounts of concentrated acids is dangerous and the reaction produces NO_x gases. For these reasons, it is critical to perform these steps in a fume hood.)** The flask was equipped with a condenser and was heated to 80 °C slowly until a vigorous reaction started. The temperature was kept at 80 °C for 30 min with stirring before being warmed to 100 °C and stirred for another 30 min. The reaction solution was cooled to room temperature and neutralized with sodium carbonate carefully to reach a pH of around 2. The product was extracted with ethyl acetate (5 × 100 ml) and the combined organic layers were washed with brine (100 ml), dried over anhydrous $MgSO_4$, and concentrated to give a viscous liquid. Chloroform (20 ml) was added to the crude product. The mixture was left at −20 °C overnight to form a crystalline precipitate, *i.e.* β-chlorolactic acid (I), as colorless plates (CCDC deposition number 2102491). The product was collected after filtration (yield 6.71 g, 54%). FT–IR [ATR (solid), cm^{-1}]: 3330 (O—H), 1739 (C═O, molecule *B*), 1708 (C═O, molecule *A*), 1090 (C—O), 674 (C—Cl). The ^{1}H NMR spectrum is in accordance with the literature (Baumruck *et al.*, 2018). HRMS (ESI): calculated for $C_3H_4{}^{35}ClO_3$ $[M - H]^-$: 122.9854, found: 122.9854. M.p. 78.7–80.8 °C. The experimental powder X-ray diffraction (PXRD) pattern matched the pattern calculated from the single-crystal data after adjusting to the (100) preferred orientation (Fig. S1 in the supporting information).

The synthesis of II was carried out according to a modified literature procedure (Patterson & O'Hagan, 2002). To a

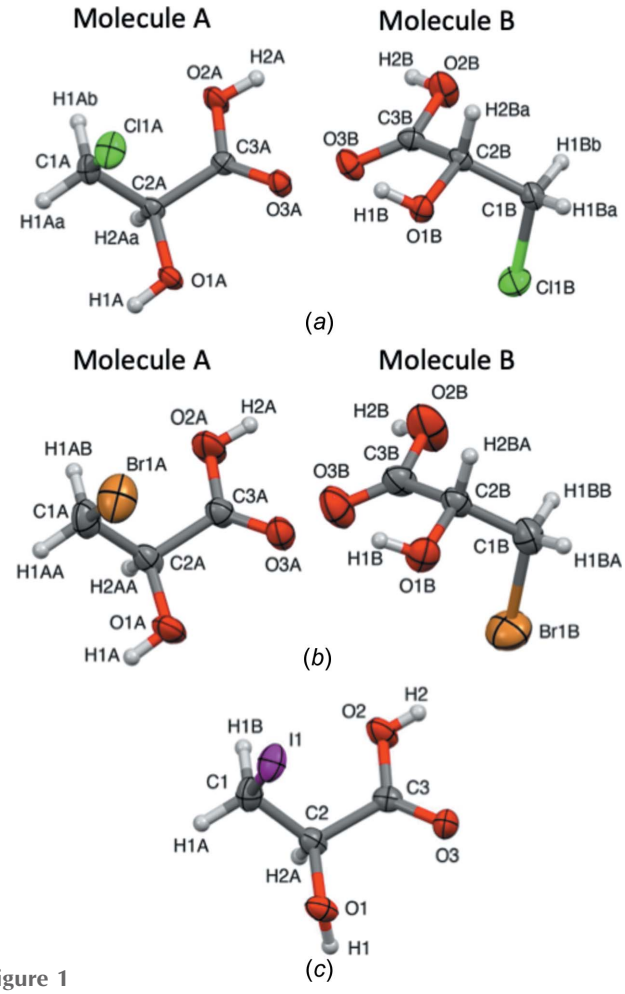

Figure 1
Views of the contents of the asymmetric units of (*a*) I, (*b*) II, and (*c*) III. Non-H atoms are drawn as 50% probability ellipsoids and H atoms as small spheres.

Table 1
Experimental details.

For all structures: monoclinic, $P2_1/c$. Experiments were carried out with Mo $K\alpha$ radiation using a Bruker Venture D8 diffractometer. Absorption was corrected for by multi-scan methods (*SADABS2016*; Bruker, 2016). H atoms were treated by a mixture of independent and constrained refinement.

	I	II	III
Crystal data			
Chemical formula	$C_3H_5ClO_3$	$C_3H_5BrO_3$	$C_3H_5IO_3$
M_r	124.52	168.98	215.97
Temperature (K)	153	301	153
a, b, c (Å)	10.8897 (7), 10.6951 (8), 9.0496 (6)	11.3076 (4), 10.8912 (3), 9.0769 (3)	11.4762 (8), 5.4370 (4), 9.1941 (7)
β (°)	108.059 (2)	106.673 (1)	92.848 (3)
V (Å^3)	1002.05 (12)	1070.85 (6)	572.97 (7)
Z	8	8	4
Z'	2	2	1
μ (mm^{-1})	0.65	7.57	5.49
Crystal size (mm)	0.22 × 0.21 × 0.08	0.4 × 0.15 × 0.06	0.27 × 0.16 × 0.06
Data collection			
T_{min}, T_{max}	0.682, 0.746	0.488, 0.746	0.556, 0.746
No. of measured, independent and observed [$I > 2\sigma(I)$] reflections	34621, 2294, 1644	25050, 2469, 2079	16586, 1308, 1102
R_{int}	0.129	0.048	0.056
(sin $\theta/\lambda)_{max}$ (Å^{-1})	0.650	0.650	0.650
Refinement			
$R[F^2 > 2\sigma(F^2)]$, $wR(F^2)$, S	0.038, 0.086, 1.00	0.039, 0.118, 1.03	0.025, 0.057, 1.10
No. of reflections	2294	2469	1308
No. of parameters	143	134	69
$\Delta\rho_{max}$, $\Delta\rho_{min}$ (e Å^{-3})	0.28, −0.32	1.28, −0.95	0.59, −0.67

Computer programs: *APEX3* (Bruker, 2016), *SAINT* (Bruker, 2016), *SHELXT2018* (Sheldrick, 2015*a*), *SHELXL2017* (Sheldrick, 2015*b*), *OLEX2* (Dolomanov *et al.*, 2009), *CrystalExplorer* (Spackman *et al.*, 2021), and *Mercury* (Macrae *et al.*, 2020).

solution of sodium borohydride (380 mg, 10.0 mmol) in water (100 ml) at 0 °C, 3-bromo-2-oxopropanoic acid (830 mg, 5.0 mmol) was added. The mixture was then stirred at room temperature for 2.5 h. 1 *M* $HCl_{(aq)}$ (20 ml) was added to the solution with stirring for 10 min, followed by extraction into ethyl acetate (4 × 40 ml). The organic layers were combined, dried over $MgSO_4$, filtered, and concentrated. The crude product was recrystallized from a mixture of CH_2Cl_2 and ether at room temperature, yielding β-bromolactic acid (II) as colorless plates (CCDC deposition number 2102492). FT–IR [ATR (solid), cm^{-1}]: 3332 (O—H), 1736 (C═O, molecule *B*), 1707 (C═O, molecule *A*), 1083 (C—O), 589 (C—Br). ^{1}H NMR [500 MHz, $(CD_3)_2CO$]: δ 4.54 (*t*, *J* = 4.1 Hz, 1H), 3.79–3.69 (*m*, 2H). HRMS (ESI): calculated for $C_3H_4{}^{79}BrO_3$ [*M* − H]$^-$: 166.9349, found: 166.9347. M.p. 78.4–81.0 °C. The experimental PXRD pattern matched the pattern calculated from the single-crystal data (Fig. S1 in the supporting information).

The synthesis of III was carried out according to a modified literature procedure (Baer & Fischer, 1949). A solution of β-chlorolactic acid (I) (623 mg, 5.00 mmol, 1.00 equiv.) and anhydrous sodium iodide (1.13 g, 7.50 mmol, 1.50 equiv.) in dry acetone (4.0 ml) was refluxed at 65 °C for 24 h. The mixture was cooled to room temperature, filtered, and the solid residue was washed with acetone again. The combined filtrate was concentrated and dissolved in acetone (4.0 ml), to which was added a second portion of anhydrous sodium iodide (1.13 g, 7.50 mmol, 1.50 equiv.). The mixture was stirred at 65 °C for another 24 h. The reaction was cooled to room temperature, filtered, and the solid residue was washed with acetone again. The combined filtrate was concentrated and then dissolved in water (10 ml). Saturated $Na_2SO_{3(aq)}$ solution (20 ml) was added to make the brown solution colorless. After acidifying with 1 *M* H_2SO_4 to pH = 2, the resulting solution was washed with hexane (2 × 20 ml), followed by extraction with ethyl ether (5 × 20 ml). The organic layers were combined, dried over $MgSO_4$, filtered, and concentrated. The crude product was dissolved in a small portion of ether and then mixed with chloroform (10 ml). The mixture was left at −20 °C overnight to form a crystalline precipitate, *i.e.* β-iodolactic acid (III), as colorless plates (CCDC deposition number 2102493). The product was collected after filtration (yield 421 mg, 39%). FT–IR [ATR (solid), cm^{-1}]: 3390 (O—H), 2902 (C—H), 1703 (C═O), 1080 (C—O), 500 (C—I). ^{1}H NMR (600 MHz, DMSO-d_6): δ 12.81 (*s*, 1H), 5.75 (*s*, 1H), 4.12 (*t*, *J* = 5.0 Hz, 1H), 3.38 (*dd*, *J* = 4.9, 3.5 Hz, 2H). HRMS (ESI): calculated for $C_3H_4IO_3$ [*M* − H]$^-$: 214.9211, found: 214.9205. M.p. 96.2–88.2 °C. The experimental PXRD pattern matched the pattern calculated from the single-crystal data after adjusting to the (100) preferred orientation (Fig. S1 in the supporting information).

2.2. Refinement

Crystal data, data collection and structure refinement details are summarized in Table 1. All H atoms bound to C atoms were placed in calculated positions and refined in riding mode, with U_{iso}(H) values set to 1.2U_{eq}(C). H atoms bound to O atoms had their positions refined freely when possible, while others required them to be restrained as riding atoms allowed

Table 2
Selected torsion angles (°).

	C1—C2—O1—H1	O3—C3—C2—O1
I, molecule *A*	57.4 (17)	−5.6 (2)
I, molecule *B*	−179 (2)	−5.6 (2)
II, molecule *A*	58.4 (4)	−4.6 (4)
II, molecule *B*	−168.8 (3)	−4.6 (4)
III	139.9 (3)	6.6 (5)

to rotate freely. For these latter H atoms, U_{iso}(H) values were set at 1.5U_{eq}(O).

3. Results and discussion

3.1. Structure

The title compounds are α-hydroxycarboxylic acids of the formula $C_3H_5XO_3$, with a halogen atom at the β-position [*X* = Cl (I), Br (II), and I (III)]. They all crystallize in the monoclinic space group $P2_1/c$. In I and II, the asymmetric unit contains two independent molecules (Z' = 2), denoted herein as I*A* and I*B* for I, and II*A* and II*B* for II (Fig. 1). The main difference between the two molecules is the direction of the hydrogen bond from the alcohol O1 atom. This hydrogen bond in molecule *A* points towards atom O1*B* of the neighboring *B* molecule, while for molecule *B*, this hydrogen bond points to atom O3*A* of the neighboring *A* molecule. Compound III has a single molecule in its asymmetric unit (Z' = 1), with its alcohol group hydrogen bonding with atom O3. A comparison of the directionality of this alcohol group is shown in Fig. S2 of the supporting information. The C1—C2—O1—H1 torsion angles (with respective *A*/*B* labels for I and II) have been tabulated (Table 2) as a quantitative measure of this directionality.

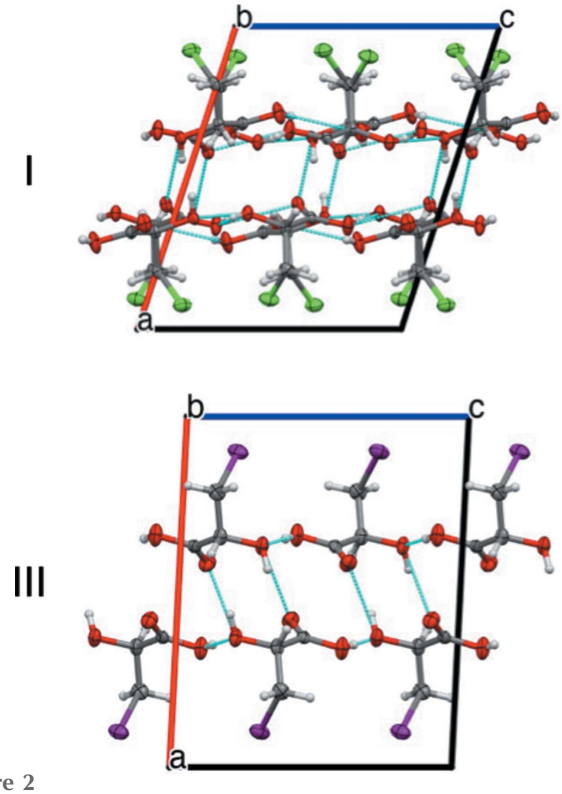

Figure 2
Packing and hydrogen bonding in I and III, viewed down the *b* axis. Halolactic acid II (not shown) is isostructural with I. Further packing and hydrogen-bonding views can be found in Fig. S3 in the supporting information.

Table 3
Hydrogen-bond geometry (Å, °).

Hydrogen-bond ID	*D*—H···*A*	*D*—H	H···*A*	*D*···*A*	*D*—H···*A*
I					
a	O1*A*—H1*A*···O1*B*^{i}	0.80 (2)	1.96 (2)	2.752 (2)	170 (2)
b	O2*A*—H2*A*···O3*A*^{ii}	0.82 (3)	2.44 (3)	2.959 (2)	122 (3)
c	O2*A*—H2*A*···O1*A*^{ii}	0.82 (3)	1.97 (3)	2.770 (2)	166 (3)
d	O1*B*—H1*B*···O3*A*	0.81 (3)	1.95 (3)	2.723 (2)	159 (3)
e	O2*B*—H2*B*···O1*B*^{ii}	0.83 (3)	2.24 (3)	3.047 (2)	164 (3)
II					
a	O1*A*—H1*A*···O1*B*^{i}	0.820 (3)	1.964 (3)	2.771 (3)	167.7 (2)
b	O2*A*—H2*A*···O3*A*^{ii}	0.820 (3)	2.427 (3)	2.974 (3)	125.1 (2)
c	O2*A*—H2*A*···O1*A*^{ii}	0.820 (3)	2.034 (2)	2.823 (4)	161.1 (3)
d	O1*B*—H1*B*···O3*A*	0.820 (3)	1.984 (2)	2.770 (4)	160.4 (2)
e	O2*B*—H2*B*···O1*B*^{ii}	0.76 (8)	2.47 (8)	3.118 (4)	145 (7)
III					
a	O1—H1···O3^{i}	0.840 (2)	1.900 (2)	2.728 (3)	168.8 (2)
b	O2—H2···O1^{ii}	0.72 (6)	1.97 (6)	2.684 (4)	172 (7)

Symmetry codes for I: (i) $-x+1, y-\frac{1}{2}, -z+\frac{1}{2}$; (ii) $x, -y+\frac{1}{2}, z-\frac{1}{2}$. Symmetry codes for II: (i) $-x+1, y-\frac{1}{2}, -z+\frac{3}{2}$; (ii) $x, -y+\frac{1}{2}, z-\frac{1}{2}$. Symmetry codes for III: (i) $x, -y+\frac{1}{2}, z-\frac{1}{2}$; (ii) $-x+1, y-\frac{1}{2}, -z+\frac{1}{2}$.

These torsion angles show the same conformation for the *A* molecules of I and II. Likewise, the *B* molecules of I and II have the same conformation, and thus the overall structures of I and II are isostructural. The molecule in III has a C1—C2—O1—H1 torsion angle of 139.9 (3)°, which is intermediate between molecules *A* and *B* of I and II, although closer to *B*. The α-hydroxy acid motif is nearly planar in all structures, with the O3—C3—C2—O1 torsion angles ranging from −5.6 (2) to 6.6 (5)° (Table 2). Additionally, the α-hydroxy group is *cis* to the C=O group of the acid, which is typical of α-hydroxy acids (Schouten *et al.*, 1994).

3.2. Hydrogen-bonding networks

The molecules in each structure are associated *via* hydrogen-bonding networks. In each molecule, there are two

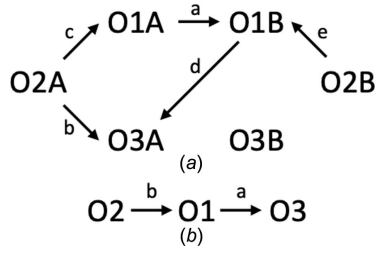

Figure 3
Schematic of the hydrogen-bonding networks of (*a*) I and II, and (*b*) III, where arrows are from the hydrogen-bond donor to the acceptor. Lowercase letters aside arrows refer to the hydrogen-bond ID used in Tables 3, 4, and 5. Note that O atoms are on unique symmetry-generated molecules.

Table 4
Unitary motifs (on-diagonal) and basic binary graph sets (off-diagonal) for I and II.

Type of hydrogen bond	a O1*A*—H1*A*···O1*B*	b O2*A*—H2*A*···O3*A*	c O2*A*—H2*A*···O1*A*	d O1*B*—H1*B*···O3*A*	e O2*B*—H2*B*···O1*B*
a O1*A*—H1*A*···O1*B*	*D*				
b O2*A*—H2*A*···O3*A*	$D_3^3(13)$	*C*(4)			
c O2*A*—H2*A*···O1*A*	$D_3^3(10)$	$C_2^2(9)[R_1^2(5)]$	*C*(5)		
d O1*B*—H1*B*···O3*A*	$C_2^2(7)$	$D_3^2(7)$	$D_3^3(10)$	*D*	
e O2*B*—H2*B*···O1*B*	$D_3^2(8)$	*	*	$D_3^3(10)$	*C*(5)

Note: (*) no link at the binary level.

hydrogen-bond donors *via* the α-hydroxy H atom on O1 and the acidic H atom on O2. Three O atoms serve as potential hydrogen-bond acceptors, although not all serve this purpose, as will be discussed. Analysis of the hydrogen-bond networks of I and II (Table 3) shows that I and II are isostructural, while III has altered connectivity.

The packing of the molecules (Fig. 2, and Fig. S3 in the supporting information) gives a bilayer of molecules connected by intermolecular hydrogen bonds in the *bc* plane. The hydrogen bonds are determined to be of moderate strength based on the bond lengths and angles (Jeffrey, 1997). The large halogen atoms are pushed away from the O—H···O hydrogen-bonded network, forming pseudo-hexagonally close-packed bilayers of halogen–halogen interactions. The layered crystal structures likely give rise to the plate-like shape of the single crystals.

The hydrogen bonds alternate between the carboxylic acid and alcohol groups, forming complex networks (Brock & Duncan, 1994). In III, hydrogen bonds form intermolecular O1—H1···O3 and O2—H2···O1 interactions creating $C_4^4(16)[R_4^4(12)]$ chains.

In I and II, molecules *A* and *B* each have unique hydrogen-bonding interactions. They have similar O2*A*—H2*A*···O1*A* and O2*B*—H2*B*···O1*B* interactions, but differ in the directionality of the H atom on O1 (Fig. 3). In *A*, the hydrogen bond is O1*A*—H1*A*···O1*B*, while for *B*, the hydrogen bond is O1*B*—H1*B*···O3*A*. There is an additional weak O2*A*—H2*A*···O3*A* hydrogen bond not present in the *B* molecule. Interestingly, O3*A* serves as an acceptor for two hydrogen bonds, while O3*B* does not participate in hydrogen bonding, which breaks Etter's first rule stating that all good hydrogen-bond donors and acceptors are involved in hydrogen bonding (Etter, 1990).

Graph-set analysis (Bernstein *et al.*, 1995; Etter *et al.*, 1990; Etter, 1990) shows that I and II have a unitary graph set, $\mathbf{N_1}$ = *DDC*(4)*C*(5)*C*(5) and a binary graph set, $\mathbf{N_2} = C_2^2(7)C_2^2(9)[R_1^2(5)]D_3^2(7)D_3^2(8)D_3^3(10)D_3^3(10)D_3^3(10)D_3^3(13)$ (Table 4). Note that, because there are five unique hydrogen bonds, there are higher-degree graph sets ($\mathbf{N_3}$, $\mathbf{N_4}$, and $\mathbf{N_5}$) not explored here. For structure III, the graph sets of degree one and two are $\mathbf{N_1}$ = *C*(5)*C*(5) and $\mathbf{N_2} = C_4^4(16)[R_4^4(12)]$ (Table 5).

Table 5
Unitary motifs (on-diagonal) and basic binary graph sets (off-diagonal) for III.

Type of hydrogen bond	a O1—H1···O3	b O2—H2···O1
a O1—H1···O3	*C*(5)	
b O2—H2···O1	$C_4^4(16)[R_4^4(12)]$	*C*(5)

4. Hirshfeld surface analysis

The Hirshfeld surface is a useful tool to partition crystalline electron density into individual molecular units (Spackman & Jayatilaka, 2009; Spackman *et al.*, 2021). The normalized contact distance, d_{norm}, can be plotted on the Hirshfeld surface using a red–white–blue color palette, where red indicates regions where d_{norm} is negative [shorter than the van der Waals (vdW) separation], white indicates regions where d_{norm} is zero (equal to the vdW separation), and blue indicates regions where d_{norm} is positive (longer than the vdW separation) (ranges are tabulated in Table S1 in the supporting information) (McKinnon *et al.*, 2007). Areas in red are of particular importance in the analysis of hydrogen bonding and highlight the intermolecular attractions between molecules in the crystal. The Hirshfeld surfaces can be converted to two-dimensional (2D) fingerprint plots, d_e *versus* d_i, where d_e and d_i represent the distance from the Hirshfeld surface to the nearest external and internal atom, respectively. In these plots, the color represents the frequency of this combination of d_e and d_i, from blue (few points) to green to red (many points), with white as zero (Spackman & McKinnon, 2002).

The Hirshfeld surfaces and 2D fingerprint plots for I*A*, I*B*, II*A*, II*B*, and III have been constructed (Fig. 4), along with the packing of the Hirshfeld surfaces (Fig. S4 in the supporting information). Red regions of the Hirshfeld surfaces correspond to hydrogen-bond donors and acceptors (for list, see Table 3), where the nearest atoms are shorter than the van der Waals separation. Of note is the α-hydroxy H atom, H1, bonded to O1. Its directionality alters the location of the nearest close contact (red region). Atom O1*A* of I and II shows two regions with short close contacts, one in the direction of H1*A* as a hydrogen-bond donor (labeled 1; hydrogen-bond ID a) and one as a hydrogen-bond acceptor (labeled 2; hydrogen-bond ID c). Atom O1*B* of I and II shows three regions of short contacts, one in the direction of H1*B* as a hydrogen-bond donor (labeled 3; hydrogen-bond ID d) and two as hydrogen-bond acceptors. One (labeled 4; hydrogen-bond ID a) is clearly stronger than the other (labeled 5; hydrogen-bond ID e), which is indicated by the intensity of the red spot. The weaker nature of this hydrogen bond is confirmed by its longer bond length. Another noticeable

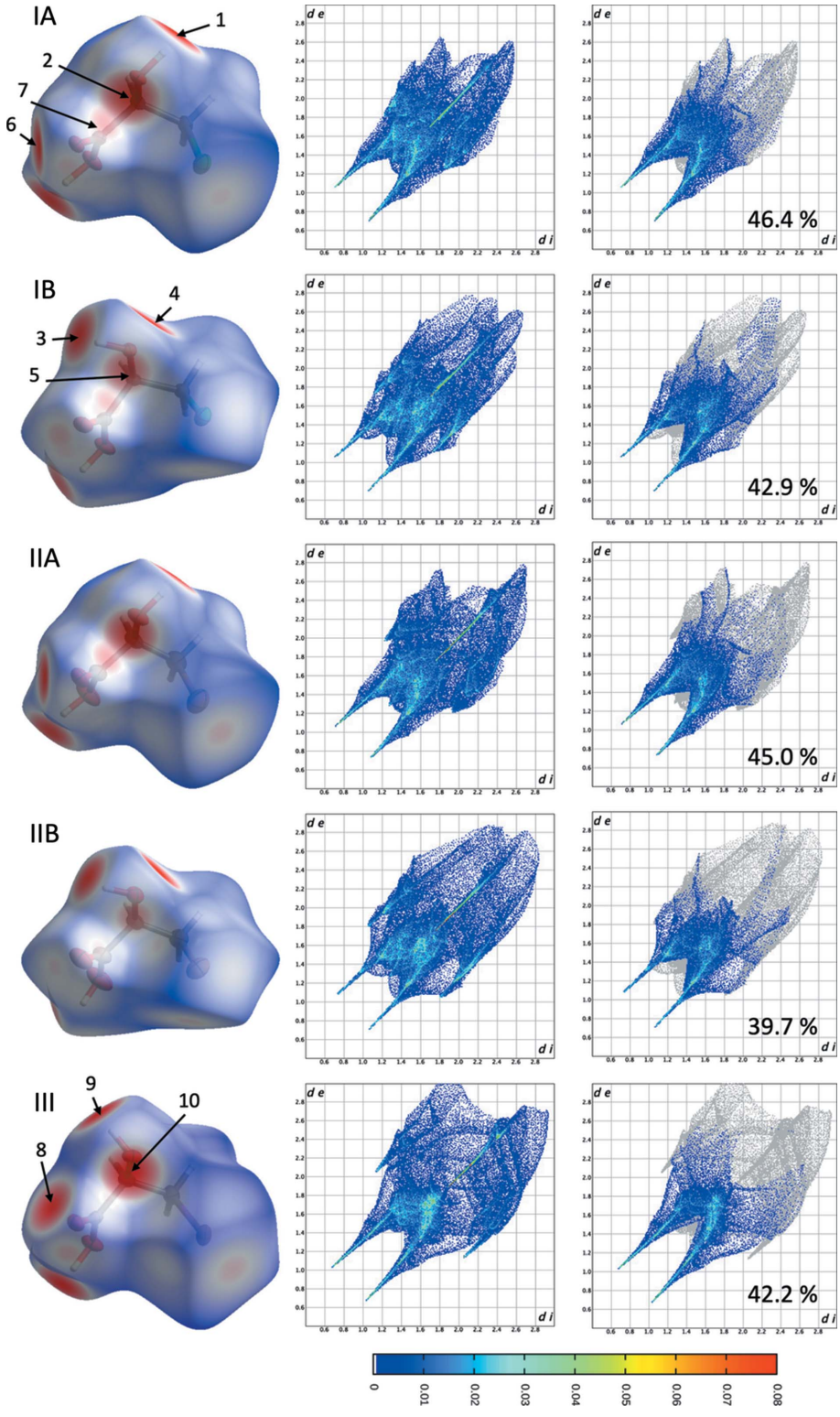

Figure 4
Views of the Hirshfeld surfaces (left) for each molecule colored to represent d_{norm}. Red areas have a negative d_{norm} where contacts are shorter than the vdW separation, white areas have a near zero d_{norm} where contacts are near the vdW separation, and blue areas have a positive d_{norm} where contacts are longer than the vdW separation. Marked spots 1–10 are discussed in the text. In the middle are the 2D fingerprint plots (d_e *versus* d_i) corresponding to the Hirshfeld surfaces on the left. On the right are the decomposed 2D fingerprint plots only coloring O···H and H···O contacts, while the others are in grey. The inset number is the percentage of these contacts compared to all contacts. The color bar at bottom applies to all 2D fingerprint plots, where the color bar represents the percentage of the total surface. Axes units are in Å for all 2D fingerprint plots.

difference in the Hirshfeld surfaces of molecules *A* and *B* of I and II is the hydrogen bond to atom O3. The two close contacts on O3*A* (labeled 6; hydrogen-bond ID d; and labeled 7; hydrogen-bond ID b) are significantly brighter red (stronger) than the same regions in molecule *B* of I and II, which are not close enough to be considered hydrogen bonds.

Comparing the short contact regions of III to I and II, there are clear differences. There is a single hydrogen bond towards O3 (labeled 8; hydrogen-bond ID a), as opposed to the two in molecule *A* and zero in molecule *B* of I and II. Atom O1 on III is a single hydrogen-bond donor (labeled 9; hydrogen-bond ID a) and single hydrogen-bond acceptor (labeled 10; hydrogen-bond ID b), similar to O1*A* in I and II; however, the donor bond points in a direction closer to O1*B* in I and II (see earlier discussion of this torsion angle).

It is worth commenting as well on the Hirshfeld surface in the region of the halogen atoms. A weak red spot opposite the C1—*X*1 connection is present in III and molecules *A* of I and II, indicating close contacts between the halogen atoms. This spot is absent in the *B* molecules of I and II. The *X*1*A*···*X*1*B* bond (or *X*1···*X*1 distance for III) lengthens with respect to the halogen atomic size, *i.e.* I [3.7858 (4) Å] > Br [3.5469 (7) Å] > Cl [3.4248 (10) Å], as would be expected, and these *X*···*X* close contacts are shorter than the sum of the vdW radii for each halogen (symmetry codes: $x+1, y, z$ for I; $x-1, y, z$ for II; $-x, y-\frac{1}{2}, -z+\frac{1}{2}$ for III). The C1*A*—*X*1*A*···*X*1*B* angles of I and II have a near linear interaction [173.48 (9) and 173.63 (11)°, respectively], while the opposite C1*B*—*X*1*B*···*X*1*A* angles are more bent [125.77 (9) and 125.69 (12)° for I and II, respectively]. Despite having an asymmetric unit with $Z' = 1$, the bond angle trends are consistent in III, with one C1—I1···I1 angle at 178.99 (10)°, and the other at 87.76 (10)°, the latter being bent more significantly.

Using the 2D fingerprint plots of the three-dimensional (3D) Hirshfeld surfaces in Fig. 4, we can now visualize the total intermolecular interactions of the

molecules and further decompose them into individual element–element contributions. Overall, these plots have defining features that can be explained. Most notably are the sharp regions pointing to the bottom left of the plots. These are the hydrogen-bonding interactions between the O and H atoms, where the upper sharp region shows hydrogen-bond donors ($d_e > d_i$) and the lower sharp region shows hydrogen-bond acceptors ($d_e < d_i$) . This area is noticeably thinner for the *B* molecules of I and II compared to the *A* molecules. The shortest contact ($d_e + d_i$) in all structures is found in III around 1.70 Å. These are larger for I at 1.74 Å and II at 1.78 Å.

Decomposing the overall 2D fingerprint plot allows us to look only at the H···O/O···H contributions (Fig. 4, right column). These are by far the most common of all the interactions on the Hirshfeld surface at nearly 50% (Table 6). The percentage decreases with the trend I*A* > II*A* > I*B* > III > II*B*, indicating that the *A* molecules are more involved in hydrogen bonding. This finding agrees with the schematic in Fig. 3 showing that *A* molecules are involved in donating and accepting three hydrogen bonds, while *B* molecules donate and accept two hydrogen bonds. The reduced H···O/O···H contributions in the *B* molecules are replaced with H···H interactions which are greater for the *B* molecules compared to *A* molecules.

The highest frequency data points (red through green) in each plot are found in a thin strip along the diagonal ($d_e = d_i$) corresponding to the halogen–halogen interaction (Fig. S5 in the supporting information). As expected, this line shifts towards longer d_e and d_i with increasing halogen size. The percent contribution of halogen–halogen interactions, *X*···*X*, to the total Hirshfeld surfaces increases with atomic size, with minor differences between the *A* and *B* molecules. This observation makes sense due to the larger halogens having longer-range orbital interactions to interact with neighboring halogen atoms.

Lastly, the 2D fingerprint plots additionally display sharp regions of H···*X*/*X*···H contacts, which appear similar to the hydrogen-bonding regions in that they point to the bottom left of the plots; however, these regions are at higher d_e and d_i values. These are most noticeable in structure III at (d_i, d_e) = (2.05, 1.15) and (1.15, 2.05). These 'wings' are present in the *A* and *B* molecules of I and II; however, they are more overlapped with other interactions. Fig. S4 shows these contacts individually.

5. Database survey

Halolactic acids I, II, and III can be compared to the parent unhalogenated L-(+)-lactic acid structure and its polymorphs [Cambridge Structural Database (CSD; Groom *et al.*, 2016) refcodes YILLAG (Schouten *et al.*, 1994), YILLAG01, YILLAG02, and YILLAG03 (Yang *et al.*, 2021)]. These all crystallize in the orthorhombic space group $P2_12_12_1$. YILLAG and YILLAG01 show 3D networks of hydrogen bonding with $Z' = 1$, while YILLAG02 has a 2D hydrogen-bonding network along the *ab* plane with $Z' = 1$. YILLAG03 has one-dimensional (1D) hydrogen bonding down the *a* axis with $Z' = 2$.

Table 6
Individual element-element interactions as percentages (%) of the total Hirshfeld surface area.

	I*A*	I*B*	II*A*	II*B*	III
H···O/O···H	46.4	42.9	45.0	39.7	42.2
H···*X*/*X*···H	25.3	25.0	25.5	28.0	27.3
H···H	15.6	19.8	16.1	19.7	16.1
X···*X*	7.0	7.1	8.3	8.2	9.3
X···O/O···*X*	2.0	1.7	1.4	0.0	2.0
O···O	1.2	1.6	1.4	2.7	1.5
O···C/C···O	1.4	1.4	1.4	1.3	0.4
H···C/C···H	1.1	0.6	1.0	0.4	0.7
C···C	0.0	0.0	0.0	0.0	0.5
X···C/C···*X*	0.0	0.0	0.0	0.0	0.0

Other related structures in the CSD include 3-chloropropionic acid (CSD refcode EREBIP; Hosten & Betz, 2021), which similarly has the space group $P2_1/c$ and $Z' = 2$. It has an analogous 2D layered hydrogen-bonded network, although along the *ab* plane. An (*S*)-3,3,3-trichlorolactate anion crystallizes with a (+)-(*S*)-1-phenylethylammonium cation (CSD refcode CEFZUJ; Takahashi *et al.*, 2006) in the space group $P2_1$, which leads to a 1D hydrogen-bonding network along the *b* axis.

The effect of halogen substitution on the resulting crystal structure has been explored previously. Three halide salts of L-asparagine monohydrate $C_4H_9N_2O_3^+\cdot X^-\cdot H_2O$, where *X* = Cl, Br, and I, have also been determined (CSD refcodes LIRLUW, LIRMAD, and LIRMEH; de Moraes *et al.*, 2018), representing a similar organic small-molecule halide series. However, all three of the halide salts were determined to be isostructural, in contrast to our results.

Three cyclic coordination clusters, $[Fe_6Dy_3(\mu\text{-OMe})_9(\text{vanox})_6(X\text{-benz})_6]$, with *X* = F, Cl, and Br (CSD refcodes QUVJEZ, QUVJID, and QUVJOJ; Kühne *et al.*, 2020), showed that the fluoro- and chloro-substituted molecules crystallized isostructurally, while the bromo-substituted analog exhibited structural distortion leading to an altered magnetic behavior.

Sterically corded pincers, PCPPd*X* (*X* = Cl, Br, and I, with CSD refcodes YARLUA, YARMEL, and YARMUB, respectively; Johnson *et al.*, 2012), were studied as halogen-bond acceptors to I_2, and showed that the chloro- and bromo-substituted complexes were isomorphous, while the iodo-substituted analog had altered bond angles and a new interaction, leading to an altered packing arrangement.

6. Conclusion

Through this work, we have determined the crystal structures of three β-halolactic acids and explored the effect of halogen substitution on the resulting hydrogen-bonding networks. It was found that all three structures crystallize in the space group $P2_1/c$, however, with differing Z'. Structures I and II have $Z' = 2$, while III crystallizes with $Z' = 1$. The difference between the two molecules in the asymmetric unit of I and II is the rotation of the H atom around the alcohol group, leading to different hydrogen-bonding networks. The *A* molecule of I and II donates and accepts three hydrogen bonds, while the *B* molecule donates and accepts two hydrogen bonds. The

Hirshfeld surfaces and 2D fingerprint plots of the structures confirm these findings, showing higher H···O/O···H contributions for the *A* molecules. We speculate that the difference in Z' is ultimately attributed to this change in the hydrogen-bonding networks. As the halogen size decreases, the symmetry of the crystal lowers and it adopts two independent molecular conformations. This minimizes the energy of the system by having one molecule donate and accept an additional hydrogen bond.

Acknowledgements

This work would not have been possible without significant discussions and contributions by Dr Maren Pink and Dr Veronica Carta. The authors thank the IU Molecular Structure Center, IU Nuclear Magnetic Resonance Facility, IU Mass Spectrometry Facility, and Professor David Williams for access to instrumentation and training. MNG thanks Kaustav Chatterjee and Stanna K. Dorn for useful discussions.

Funding information

Funding for this research was provided by: National Science Foundation – Division of Materials Research (grant No. 2113536); Major Scientific Research Equipment Fund from the President of Indiana University and the Office of the Vice President for Research (award to Dr Maren Pink).

References

Baer, E. & Fischer, H. O. (1949). *J. Biol. Chem.* **180**, 145–154.
Baumruck, A., Tietze, D., Steinacker, L. & Tietze, A. (2018). *Chem. Sci.* **9**, 2365–2375.
Bernstein, J., Davis, R. E., Shimoni, L. & Chang, N.-L. (1995). *Angew. Chem. Int. Ed. Engl.* **34**, 1555–1573.
Brock, C. P. & Duncan, L. L. (1994). *Chem. Mater.* **6**, 1307–1312.
Bruker (2016). *APEX3*, *SAINT*, and *SADABS*. Bruker AXS Inc., Madison, Wisconsin, USA.
Dolomanov, O. V., Bourhis, L. J., Gildea, R. J., Howard, J. A. K. & Puschmann, H. (2009). *J. Appl. Cryst.* **42**, 339–341.
Etter, M. C. (1990). *Acc. Chem. Res.* **23**, 120–126.
Etter, M. C., MacDonald, J. C. & Bernstein, J. (1990). *Acta Cryst.* B**46**, 256–262.
Gavezzotti, A. (2008). *CrystEngComm*, **10**, 389–398.
Groom, C. R., Bruno, I. J., Lightfoot, M. P. & Ward, S. C. (2016). *Acta Cryst.* B**72**, 171–179.
Hosten, E. C. & Betz, R. (2021). *Z. Kristallogr. New Cryst. Struct.* **236**, 273–275.
Inkinen, S., Hakkarainen, M., Albertsson, A.-C. & Södergård, A. (2011). *Biomacromolecules*, **12**, 523–532.
Jeffrey, G. A. (1997). *An Introduction to Hydrogen Bonding*, p. 12. New York: Oxford University Press Inc.
Johnson, M. T., Džolić, Z., Cetina, M., Wendt, O. F., Öhrström, L. & Rissanen, K. (2012). *Cryst. Growth Des.* **12**, 362–368.
Kühne, I. A., Anson, C. E. & Powell, A. K. (2020). *Front. Chem.* **8**, 701.
Macrae, C. F., Sovago, I., Cottrell, S. J., Galek, P. T. A., McCabe, P., Pidcock, E., Platings, M., Shields, G. P., Stevens, J. S., Towler, M. & Wood, P. A. (2020). *J. Appl. Cryst.* **53**, 226–235.
McKinnon, J. J., Jayatilaka, D. & Spackman, M. A. (2007). *Chem. Commun.* pp. 3814–3816.
Moraes, L. S. de, Kennedy, A. R. & Logan, C. R. (2018). *Acta Cryst.* E**74**, 1619–1623.
Patterson, S. & O'Hagan, D. (2002). *Phytochemistry*, **61**, 323–329.
Sayre, H., Milos, K., Goldcamp, M. J., Schroll, C. A., Krause, J. A. & Baldwin, M. J. (2010). *Inorg. Chem.* **49**, 4433–4439.
Schouten, A., Kanters, J. A. & van Krieken, J. (1994). *J. Mol. Struct.* **323**, 165–168.
Sheldrick, G. M. (2015*a*). *Acta Cryst.* A**71**, 3–8.
Sheldrick, G. M. (2015*b*). *Acta Cryst.* C**71**, 3–8.
Souaya, E. R., Khalil, M. M. H., Ismail, E. H., Bendas, E. R. & Neaz, O. S. (2014). *Res. J. Pharm. Biol. Chem. Sci.* **5**, 18–30.
Spackman, M. A. & Jayatilaka, D. (2009). *CrystEngComm*, **11**, 19–32.
Spackman, M. A. & McKinnon, J. J. (2002). *CrystEngComm*, **4**, 378–392.
Spackman, P. R., Turner, M. J., McKinnon, J. J., Wolff, S. K., Grimwood, D. J., Jayatilaka, D. & Spackman, M. A. (2021). *J. Appl. Cryst.* **54**, 1006–1011.
Steed, K. M. & Steed, J. W. (2015). *Chem. Rev.* **115**, 2895–2933.
Takahashi, S., Jukurogi, T., Katagiri, T. & Uneyama, K. (2006). *CrystEngComm*, **8**, 320–326.
Tang, S.-C. & Yang, J.-H. (2018). *Molecules*, **23**, 863.
Yang, J., Hu, C. T., Reiter, E. & Kahr, B. (2021). *CrystEngComm*, **23**, 2644–2647.

supporting information

Acta Cryst. (2022). C**78**, 257-264 [https://doi.org/10.1107/S2053229622002856]

Crystal structures of three *β*-halolactic acids: hydrogen bonding resulting in differing *Z′*

Matthew N. Gordon, Yanyao Liu, Ibrahim H. Shafei, M. Kevin Brown and Sara E. Skrabalak

Computing details

For all structures, data collection: *APEX3* (Bruker, 2016); cell refinement: *SAINT* (Bruker, 2016); data reduction: *SAINT* (Bruker, 2016); program(s) used to solve structure: SHELXT2018 (Sheldrick, 2015*a*); program(s) used to refine structure: *SHELXL2017* (Sheldrick, 2015*b*); molecular graphics: OLEX2 (Dolomanov *et al.*, 2009); software used to prepare material for publication: OLEX2 (Dolomanov *et al.*, 2009), *Mercury* (Macrae *et al.*, 2020) and CrystalExplorer (Spackman *et al.*, 2021).

3-Chloro-2-hydroxypropanoic acid (21165)

Crystal data

$C_3H_5ClO_3$
M_r = 124.52
Monoclinic, $P2_1/c$
a = 10.8897 (7) Å
b = 10.6951 (8) Å
c = 9.0496 (6) Å
β = 108.059 (2)°
V = 1002.05 (12) Å^3
Z = 8
$F(000)$ = 512
D_x = 1.651 Mg m^{-3}
Mo $K\alpha$ radiation, λ = 0.71073 Å
Cell parameters from 4811 reflections
θ = 3.0–26.0°
μ = 0.65 mm^{-1}
T = 153 K
Plate, colourless
0.22 × 0.21 × 0.08 mm

Data collection

Bruker Venture D8 diffractometer
φ and ω scans
Absorption correction: multi-scan (SADABS2016; Bruker, 2016)
T_{min} = 0.682, T_{max} = 0.746
34621 measured reflections
2294 independent reflections
1644 reflections with $I > 2\sigma(I)$
R_{int} = 0.129
θ_{max} = 27.5°, θ_{min} = 2.7°
h = −14→13
k = −13→13
l = −11→11

Refinement

Refinement on F^2
Least-squares matrix: full
$R[F^2 > 2\sigma(F^2)]$ = 0.038
$wR(F^2)$ = 0.086
S = 1.00
2294 reflections
143 parameters
0 restraints
Hydrogen site location: mixed
H atoms treated by a mixture of independent and constrained refinement
$w = 1/[\sigma^2(F_o^2) + (0.0371P)^2 + 0.3727P]$ where $P = (F_o^2 + 2F_c^2)/3$
$(\Delta/\sigma)_{max}$ = 0.001
$\Delta\rho_{max}$ = 0.28 e Å^{-3}
$\Delta\rho_{min}$ = −0.32 e Å^{-3}

Special details

Geometry. All e.s.d.'s (except the e.s.d. in the dihedral angle between two l.s. planes) are estimated using the full covariance matrix. The cell e.s.d.'s are taken into account individually in the estimation of e.s.d.'s in distances, angles and torsion angles; correlations between e.s.d.'s in cell parameters are only used when they are defined by crystal symmetry. An approximate (isotropic) treatment of cell e.s.d.'s is used for estimating e.s.d.'s involving l.s. planes.

Fractional atomic coordinates and isotropic or equivalent isotropic displacement parameters (Å²)

	x	*y*	*z*	U_{iso}*/U_{eq}
Cl1A	0.90026 (6)	0.16529 (6)	0.46073 (7)	0.03398 (17)
O1A	0.61723 (15)	0.10079 (14)	0.27482 (16)	0.0223 (3)
H1A	0.630 (2)	0.044 (2)	0.224 (3)	0.023 (7)*
O2A	0.65712 (17)	0.16424 (16)	0.66921 (17)	0.0304 (4)
H2A	0.637 (3)	0.227 (3)	0.708 (3)	0.046 (8)*
O3A	0.58743 (14)	0.28048 (13)	0.45347 (16)	0.0216 (3)
C1A	0.8043 (2)	0.0385 (2)	0.4917 (3)	0.0234 (5)
H1AA	0.819542	−0.036310	0.435266	0.028*
H1AB	0.830323	0.018025	0.603828	0.028*
C2A	0.6621 (2)	0.07151 (19)	0.4356 (2)	0.0194 (4)
H2AA	0.611759	−0.001565	0.454756	0.023*
C3A	0.63140 (19)	0.18414 (19)	0.5191 (2)	0.0181 (4)
Cl1B	0.07951 (5)	0.39421 (6)	0.36033 (7)	0.03451 (17)
O1B	0.36771 (15)	0.41250 (15)	0.42619 (17)	0.0227 (4)
H1B	0.438 (3)	0.379 (3)	0.457 (3)	0.044 (8)*
O2B	0.28656 (18)	0.33943 (17)	0.76908 (19)	0.0352 (4)
H2B	0.296 (3)	0.273 (3)	0.818 (3)	0.041 (8)*
O3B	0.35042 (16)	0.21788 (14)	0.60475 (17)	0.0289 (4)
C1B	0.1898 (2)	0.4971 (2)	0.4920 (2)	0.0233 (5)
H1BA	0.196511	0.576028	0.437887	0.028*
H1BB	0.156841	0.517323	0.579555	0.028*
C2B	0.3218 (2)	0.4379 (2)	0.5540 (2)	0.0191 (4)
H2BA	0.381583	0.498914	0.624543	0.023*
C3B	0.3211 (2)	0.3181 (2)	0.6435 (2)	0.0211 (5)

Atomic displacement parameters (Å²)

	U^{11}	U^{22}	U^{33}	U^{12}	U^{13}	U^{23}
Cl1A	0.0262 (3)	0.0290 (3)	0.0477 (4)	−0.0023 (2)	0.0129 (3)	0.0052 (3)
O1A	0.0316 (9)	0.0193 (8)	0.0174 (8)	0.0009 (7)	0.0095 (7)	−0.0043 (7)
O2A	0.0516 (11)	0.0238 (9)	0.0182 (8)	0.0109 (8)	0.0144 (8)	−0.0003 (7)
O3A	0.0300 (8)	0.0169 (8)	0.0207 (8)	0.0032 (6)	0.0117 (6)	0.0016 (6)
C1A	0.0255 (11)	0.0189 (11)	0.0283 (12)	0.0028 (9)	0.0119 (10)	0.0021 (9)
C2A	0.0260 (11)	0.0171 (11)	0.0169 (10)	−0.0001 (9)	0.0095 (9)	0.0003 (8)
C3A	0.0196 (10)	0.0187 (12)	0.0176 (10)	−0.0014 (8)	0.0082 (9)	0.0007 (8)
Cl1B	0.0243 (3)	0.0377 (4)	0.0383 (3)	−0.0027 (3)	0.0049 (3)	−0.0039 (3)
O1B	0.0245 (8)	0.0270 (9)	0.0205 (8)	0.0054 (7)	0.0126 (7)	0.0036 (6)
O2B	0.0592 (12)	0.0280 (10)	0.0288 (9)	0.0098 (9)	0.0287 (9)	0.0090 (8)
O3B	0.0426 (10)	0.0180 (8)	0.0309 (9)	−0.0001 (7)	0.0182 (8)	−0.0014 (7)

C1B	0.0273 (11)	0.0198 (11)	0.0252 (11)	0.0024 (9)	0.0119 (9)	0.0001 (9)
C2B	0.0229 (11)	0.0186 (11)	0.0176 (10)	−0.0015 (8)	0.0091 (9)	−0.0009 (8)
C3B	0.0235 (11)	0.0227 (12)	0.0175 (11)	−0.0018 (9)	0.0071 (9)	0.0001 (9)

Geometric parameters (Å, º)

Cl1A—C1A	1.786 (2)	Cl1B—C1B	1.785 (2)
O1A—H1A	0.80 (2)	O1B—H1B	0.81 (3)
O1A—C2A	1.418 (2)	O1B—C2B	1.421 (2)
O2A—H2A	0.82 (3)	O2B—H2B	0.83 (3)
O2A—C3A	1.316 (2)	O2B—C3B	1.323 (2)
O3A—C3A	1.211 (2)	O3B—C3B	1.201 (2)
C1A—H1AA	0.9900	C1B—H1BA	0.9900
C1A—H1AB	0.9900	C1B—H1BB	0.9900
C1A—C2A	1.515 (3)	C1B—C2B	1.510 (3)
C2A—H2AA	1.0000	C2B—H2BA	1.0000
C2A—C3A	1.513 (3)	C2B—C3B	1.517 (3)
C2A—O1A—H1A	110.4 (16)	C2B—O1B—H1B	109.4 (19)
C3A—O2A—H2A	108 (2)	C3B—O2B—H2B	107.1 (18)
Cl1A—C1A—H1AA	109.5	Cl1B—C1B—H1BA	109.5
Cl1A—C1A—H1AB	109.5	Cl1B—C1B—H1BB	109.5
H1AA—C1A—H1AB	108.0	H1BA—C1B—H1BB	108.1
C2A—C1A—Cl1A	110.94 (15)	C2B—C1B—Cl1B	110.83 (15)
C2A—C1A—H1AA	109.5	C2B—C1B—H1BA	109.5
C2A—C1A—H1AB	109.5	C2B—C1B—H1BB	109.5
O1A—C2A—C1A	112.72 (16)	O1B—C2B—C1B	108.19 (16)
O1A—C2A—H2AA	108.5	O1B—C2B—H2BA	108.7
O1A—C2A—C3A	106.11 (16)	O1B—C2B—C3B	109.50 (17)
C1A—C2A—H2AA	108.5	C1B—C2B—H2BA	108.7
C3A—C2A—C1A	112.29 (17)	C1B—C2B—C3B	113.03 (17)
C3A—C2A—H2AA	108.5	C3B—C2B—H2BA	108.7
O2A—C3A—C2A	112.18 (18)	O2B—C3B—C2B	111.23 (18)
O3A—C3A—O2A	124.67 (19)	O3B—C3B—O2B	125.2 (2)
O3A—C3A—C2A	123.16 (18)	O3B—C3B—C2B	123.54 (18)
Cl1A—C1A—C2A—O1A	59.7 (2)	Cl1B—C1B—C2B—O1B	60.43 (19)
Cl1A—C1A—C2A—C3A	−60.1 (2)	Cl1B—C1B—C2B—C3B	−61.0 (2)
O1A—C2A—C3A—O2A	173.88 (17)	O1B—C2B—C3B—O2B	176.07 (17)
O1A—C2A—C3A—O3A	−5.6 (3)	O1B—C2B—C3B—O3B	−2.9 (3)
C1A—C2A—C3A—O2A	−62.5 (2)	C1B—C2B—C3B—O2B	−63.2 (2)
C1A—C2A—C3A—O3A	117.9 (2)	C1B—C2B—C3B—O3B	117.8 (2)

Hydrogen-bond geometry (Å, º)

D—H···*A*	*D*—H	H···*A*	*D*···*A*	*D*—H···*A*
O1*A*—H1*A*···O1*B*^{i}	0.80 (2)	1.96 (2)	2.752 (2)	170 (2)
O2*A*—H2*A*···O1*A*^{ii}	0.82 (3)	1.97 (3)	2.770 (2)	166 (3)

O2*A*—H2*A*···O3*A*^{ii}	0.82 (3)	2.45 (3)	2.959 (2)	121 (2)
C1*A*—H1*AA*···O3*B*^{iii}	0.99	2.63	3.195 (3)	116
C2*A*—H2*AA*···O3*B*^{iii}	1.00	2.44	3.114 (3)	124
O1*B*—H1*B*···O3*A*	0.81 (3)	1.95 (3)	2.723 (2)	159 (3)
O2*B*—H2*B*···O1*B*^{ii}	0.83 (3)	2.24 (3)	3.047 (2)	164 (2)
O2*B*—H2*B*···O3*B*^{ii}	0.83 (3)	2.47 (3)	2.963 (2)	119 (2)
C1*B*—H1*BB*···Cl1*B*^{iv}	0.99	2.95	3.764 (2)	141
C2*B*—H2*BA*···O3*A*^{v}	1.00	2.52	3.177 (3)	123

Symmetry codes: (i) −*x*+1, *y*−1/2, −*z*+1/2; (ii) *x*, −*y*+1/2, *z*+1/2; (iii) −*x*+1, −*y*, −*z*+1; (iv) −*x*, −*y*+1, −*z*+1; (v) −*x*+1, −*y*+1, −*z*+1.

3-Bromo-2-hydroxypropanoic acid (mo_21189_0ma_a)

Crystal data

$C_3H_5BrO_3$
M_r = 168.98
Monoclinic, $P2_1/c$
a = 11.3076 (4) Å
b = 10.8912 (3) Å
c = 9.0769 (3) Å
β = 106.673 (1)°
V = 1070.85 (6) Å^3
Z = 8
$F(000)$ = 656
D_x = 2.096 Mg m^{-3}
Mo $K\alpha$ radiation, λ = 0.71073 Å
Cell parameters from 9452 reflections
θ = 2.7–27.3°
μ = 7.57 mm^{-1}
T = 301 K
Plate, colourless
0.4 × 0.15 × 0.06 mm

Data collection

Bruker APEXII CCD diffractometer
φ and ω scans
Absorption correction: multi-scan (SADABS2016; Bruker, 2016)
T_{min} = 0.488, T_{max} = 0.746
25050 measured reflections
2469 independent reflections
2079 reflections with $I > 2\sigma(I)$
R_{int} = 0.048
θ_{max} = 27.5°, θ_{min} = 1.9°
h = −14→14
k = −14→14
l = −11→11

Refinement

Refinement on F^2
Least-squares matrix: full
$R[F^2 > 2\sigma(F^2)]$ = 0.039
$wR(F^2)$ = 0.118
S = 1.03
2469 reflections
134 parameters
0 restraints
Hydrogen site location: mixed
H atoms treated by a mixture of independent and constrained refinement
$w = 1/[\sigma^2(F_o^2) + (0.0662P)^2 + 1.5353P]$ where $P = (F_o^2 + 2F_c^2)/3$
$(\Delta/\sigma)_{max} < 0.001$
$\Delta\rho_{max}$ = 1.28 e Å^{-3}
$\Delta\rho_{min}$ = −0.95 e Å^{-3}

Special details

Geometry. All e.s.d.'s (except the e.s.d. in the dihedral angle between two l.s. planes) are estimated using the full covariance matrix. The cell e.s.d.'s are taken into account individually in the estimation of e.s.d.'s in distances, angles and torsion angles; correlations between e.s.d.'s in cell parameters are only used when they are defined by crystal symmetry. An approximate (isotropic) treatment of cell e.s.d.'s is used for estimating e.s.d.'s involving l.s. planes.

Fractional atomic coordinates and isotropic or equivalent isotropic displacement parameters (Å^2)

	x	*y*	*z*	U_{iso}*/U_{eq}
Br1A	0.10364 (4)	0.16899 (4)	0.54355 (6)	0.05749 (18)

Br1B	0.91376 (4)	0.39586 (5)	0.64075 (6)	0.05988 (18)
O3A	0.4161 (2)	0.2773 (2)	0.5508 (3)	0.0343 (5)
O1B	0.6270 (3)	0.4133 (2)	0.5699 (3)	0.0371 (5)
H1B	0.566391	0.368331	0.543845	0.048 (13)*
O1A	0.3836 (3)	0.1011 (2)	0.7284 (3)	0.0379 (6)
H1A	0.370903	0.042310	0.778162	0.057*
O3B	0.6459 (3)	0.2210 (2)	0.3935 (3)	0.0501 (7)
O2A	0.3537 (3)	0.1622 (3)	0.3393 (3)	0.0505 (8)
H2A	0.373757	0.222673	0.298229	0.076*
O2B	0.7047 (4)	0.3401 (3)	0.2277 (4)	0.0635 (10)
H2B	0.719 (7)	0.276 (7)	0.203 (8)	0.095*
C3A	0.3753 (3)	0.1828 (3)	0.4872 (4)	0.0292 (6)
C2A	0.3451 (3)	0.0719 (3)	0.5701 (4)	0.0302 (7)
H2AA	0.394352	0.002381	0.552467	0.036*
C2B	0.6706 (3)	0.4373 (3)	0.4414 (4)	0.0297 (6)
H2BA	0.613365	0.494429	0.373053	0.036*
C3B	0.6728 (4)	0.3190 (3)	0.3542 (4)	0.0342 (7)
C1B	0.7950 (3)	0.4981 (3)	0.4962 (4)	0.0387 (8)
H1BA	0.786612	0.575553	0.545101	0.046*
H1BB	0.825070	0.515574	0.408563	0.046*
C1A	0.2097 (4)	0.0372 (3)	0.5129 (4)	0.0396 (8)
H1AA	0.195341	−0.035446	0.567198	0.048*
H1AB	0.188908	0.017427	0.404309	0.048*

Atomic displacement parameters (Å²)

	U^{11}	U^{22}	U^{33}	U^{12}	U^{13}	U^{23}
Br1A	0.0435 (3)	0.0478 (3)	0.0813 (4)	0.00380 (17)	0.0181 (2)	−0.0083 (2)
Br1B	0.0396 (3)	0.0708 (3)	0.0643 (3)	0.00844 (19)	0.0070 (2)	0.0066 (2)
O3A	0.0491 (14)	0.0264 (11)	0.0308 (12)	−0.0073 (10)	0.0168 (11)	−0.0023 (9)
O1B	0.0428 (14)	0.0438 (13)	0.0303 (12)	−0.0075 (11)	0.0193 (11)	−0.0090 (10)
O1A	0.0561 (16)	0.0347 (12)	0.0237 (11)	−0.0012 (11)	0.0124 (11)	0.0070 (9)
O3B	0.080 (2)	0.0268 (12)	0.0506 (16)	−0.0011 (13)	0.0293 (15)	−0.0004 (11)
O2A	0.090 (2)	0.0420 (14)	0.0235 (12)	−0.0201 (14)	0.0221 (13)	−0.0021 (10)
O2B	0.113 (3)	0.0477 (17)	0.0479 (17)	−0.0128 (18)	0.0520 (19)	−0.0116 (14)
C3A	0.0372 (17)	0.0264 (14)	0.0257 (15)	0.0002 (12)	0.0119 (13)	0.0006 (11)
C2A	0.0456 (19)	0.0215 (13)	0.0273 (15)	0.0022 (12)	0.0168 (14)	0.0021 (11)
C2B	0.0388 (17)	0.0260 (14)	0.0265 (15)	0.0015 (12)	0.0129 (13)	0.0006 (11)
C3B	0.0460 (19)	0.0312 (16)	0.0277 (16)	0.0028 (14)	0.0144 (14)	−0.0017 (12)
C1B	0.043 (2)	0.0343 (17)	0.0424 (19)	−0.0029 (15)	0.0177 (16)	0.0026 (14)
C1A	0.053 (2)	0.0252 (15)	0.044 (2)	−0.0047 (14)	0.0181 (17)	−0.0063 (13)

Geometric parameters (Å, º)

Br1A—C1A	1.941 (4)	O2B—C3B	1.319 (4)
Br1B—C1B	1.938 (4)	C3A—C2A	1.512 (4)
O3A—C3A	1.206 (4)	C2A—H2AA	0.9800
O1B—H1B	0.8200	C2A—C1A	1.517 (5)

O1B—C2B	1.415 (4)	C2B—H2BA	0.9800
O1A—H1A	0.8200	C2B—C3B	1.517 (4)
O1A—C2A	1.413 (4)	C2B—C1B	1.504 (5)
O3B—C3B	1.192 (4)	C1B—H1BA	0.9700
O2A—H2A	0.8200	C1B—H1BB	0.9700
O2A—C3A	1.313 (4)	C1A—H1AA	0.9700
O2B—H2B	0.76 (8)	C1A—H1AB	0.9700
C2B—O1B—H1B	109.5	C1B—C2B—H2BA	108.4
C2A—O1A—H1A	109.5	C1B—C2B—C3B	113.2 (3)
C3A—O2A—H2A	109.5	O3B—C3B—O2B	125.0 (3)
C3B—O2B—H2B	103 (6)	O3B—C3B—C2B	124.1 (3)
O3A—C3A—O2A	124.7 (3)	O2B—C3B—C2B	110.8 (3)
O3A—C3A—C2A	123.6 (3)	Br1B—C1B—H1BA	109.3
O2A—C3A—C2A	111.7 (3)	Br1B—C1B—H1BB	109.3
O1A—C2A—C3A	106.2 (3)	C2B—C1B—Br1B	111.8 (2)
O1A—C2A—H2AA	108.4	C2B—C1B—H1BA	109.3
O1A—C2A—C1A	113.0 (3)	C2B—C1B—H1BB	109.3
C3A—C2A—H2AA	108.4	H1BA—C1B—H1BB	107.9
C3A—C2A—C1A	112.2 (3)	Br1A—C1A—H1AA	109.3
C1A—C2A—H2AA	108.4	Br1A—C1A—H1AB	109.3
O1B—C2B—H2BA	108.4	C2A—C1A—Br1A	111.8 (2)
O1B—C2B—C3B	109.6 (3)	C2A—C1A—H1AA	109.3
O1B—C2B—C1B	108.8 (3)	C2A—C1A—H1AB	109.3
C3B—C2B—H2BA	108.4	H1AA—C1A—H1AB	107.9
O3A—C3A—C2A—O1A	−4.6 (5)	O2A—C3A—C2A—O1A	174.3 (3)
O3A—C3A—C2A—C1A	119.3 (4)	O2A—C3A—C2A—C1A	−61.8 (4)
O1B—C2B—C3B—O3B	−2.7 (5)	C3A—C2A—C1A—Br1A	−60.5 (3)
O1B—C2B—C3B—O2B	175.5 (3)	C3B—C2B—C1B—Br1B	−62.6 (3)
O1B—C2B—C1B—Br1B	59.5 (3)	C1B—C2B—C3B—O3B	119.0 (4)
O1A—C2A—C1A—Br1A	59.5 (3)	C1B—C2B—C3B—O2B	−62.9 (4)

Hydrogen-bond geometry (Å, º)

D—H···*A*	*D*—H	H···*A*	*D*···*A*	*D*—H···*A*
O1*A*—H1*A*···O1*B*^{i}	0.82	1.96	2.771 (3)	168
O2*A*—H2*A*···O3*A*^{ii}	0.82	2.43	2.974 (3)	125
O2*A*—H2*A*···O1*A*^{ii}	0.82	2.03	2.823 (4)	161
O2*B*—H2*B*···Br1*B*^{ii}	0.76 (8)	3.07 (8)	3.726 (4)	146 (7)
O2*B*—H2*B*···O1*B*^{ii}	0.76 (8)	2.47 (8)	3.118 (4)	145 (7)
O2*B*—H2*B*···O3*B*^{ii}	0.76 (8)	2.70 (7)	2.988 (4)	105 (6)
C2*A*—H2*AA*···O3*B*^{iii}	0.98	2.55	3.206 (4)	124
C2*B*—H2*BA*···O3*A*^{iv}	0.98	2.63	3.265 (4)	123
C1*A*—H1*AA*···O3*B*^{iii}	0.97	2.66	3.240 (5)	119

Symmetry codes: (i) −*x*+1, *y*−1/2, −*z*+3/2; (ii) *x*, −*y*+1/2, *z*−1/2; (iii) −*x*+1, −*y*, −*z*+1; (iv) −*x*+1, −*y*+1, −*z*+1.

2-Hydroxy-3-iodopropanoic acid (21166)

Crystal data

$C_3H_5IO_3$
$M_r = 215.97$
Monoclinic, $P2_1/c$
$a = 11.4762$ (8) Å
$b = 5.4370$ (4) Å
$c = 9.1941$ (7) Å
$\beta = 92.848$ (3)°
$V = 572.97$ (7) Å^3
$Z = 4$
$F(000) = 400$
$D_x = 2.504$ Mg m^{-3}
Mo $K\alpha$ radiation, $\lambda = 0.71073$ Å
Cell parameters from 6362 reflections
$\theta = 3.6$–27.0°
$\mu = 5.49$ mm^{-1}
$T = 153$ K
Plate, colourless
0.27 × 0.16 × 0.06 mm

Data collection

Bruker APEXII CCD diffractometer
φ and ω scans
Absorption correction: multi-scan (SADABS2016; Bruker, 2016)
$T_{min} = 0.556$, $T_{max} = 0.746$
16586 measured reflections
1308 independent reflections
1102 reflections with $I > 2\sigma(I)$
$R_{int} = 0.056$
$\theta_{max} = 27.5°$, $\theta_{min} = 3.6°$
$h = -14\rightarrow14$
$k = -6\rightarrow7$
$l = -11\rightarrow11$

Refinement

Refinement on F^2
Least-squares matrix: full
$R[F^2 > 2\sigma(F^2)] = 0.025$
$wR(F^2) = 0.057$
$S = 1.10$
1308 reflections
69 parameters
0 restraints
Hydrogen site location: mixed
H atoms treated by a mixture of independent and constrained refinement
$w = 1/[\sigma^2(F_o^2) + (0.0197P)^2 + 1.2602P]$ where $P = (F_o^2 + 2F_c^2)/3$
$(\Delta/\sigma)_{max} < 0.001$
$\Delta\rho_{max} = 0.59$ e Å^{-3}
$\Delta\rho_{min} = -0.66$ e Å^{-3}

Special details

Geometry. All e.s.d.'s (except the e.s.d. in the dihedral angle between two l.s. planes) are estimated using the full covariance matrix. The cell e.s.d.'s are taken into account individually in the estimation of e.s.d.'s in distances, angles and torsion angles; correlations between e.s.d.'s in cell parameters are only used when they are defined by crystal symmetry. An approximate (isotropic) treatment of cell e.s.d.'s is used for estimating e.s.d.'s involving l.s. planes.

Fractional atomic coordinates and isotropic or equivalent isotropic displacement parameters (Å^2)

	x	y	z	U_{iso}*/U_{eq}
I1	0.10060 (2)	0.11577 (5)	0.18694 (3)	0.03582 (11)
O1	0.3689 (2)	−0.0419 (5)	0.2883 (3)	0.0280 (6)
H1	0.435419	−0.096878	0.312553	0.042*
O2	0.3384 (3)	0.0992 (5)	−0.0900 (3)	0.0337 (7)
H2	0.349 (5)	0.211 (12)	−0.130 (7)	0.07 (2)*
O3	0.4187 (2)	0.3096 (5)	0.0974 (3)	0.0314 (6)
C1	0.2156 (3)	−0.1709 (7)	0.1191 (4)	0.0303 (8)
H1A	0.202299	−0.321458	0.176539	0.036*
H1B	0.197462	−0.209631	0.015196	0.036*
C2	0.3422 (3)	−0.0953 (6)	0.1394 (4)	0.0246 (7)
H2A	0.392167	−0.235737	0.109911	0.030*

C3	0.3704 (3)	0.1277 (6)	0.0481 (4)	0.0213 (7)

Atomic displacement parameters (Å²)

	U^{11}	U^{22}	U^{33}	U^{12}	U^{13}	U^{23}
I1	0.02602 (14)	0.03541 (17)	0.04660 (17)	−0.00509 (11)	0.00755 (10)	−0.00537 (12)
O1	0.0384 (14)	0.0265 (14)	0.0186 (12)	0.0055 (11)	−0.0021 (10)	0.0007 (10)
O2	0.0570 (19)	0.0251 (15)	0.0187 (13)	−0.0030 (13)	0.0000 (12)	0.0011 (12)
O3	0.0349 (14)	0.0280 (14)	0.0307 (14)	−0.0105 (11)	−0.0036 (11)	0.0033 (11)
C1	0.034 (2)	0.025 (2)	0.033 (2)	−0.0055 (15)	0.0048 (16)	−0.0041 (15)
C2	0.0328 (19)	0.0201 (18)	0.0209 (17)	0.0033 (14)	0.0017 (14)	−0.0009 (14)
C3	0.0208 (15)	0.0234 (18)	0.0199 (16)	0.0058 (14)	0.0027 (12)	−0.0015 (14)

Geometric parameters (Å, º)

I1—C1	2.154 (4)	C1—H1A	0.9900
O1—H1	0.8400	C1—H1B	0.9900
O1—C2	1.418 (4)	C1—C2	1.513 (5)
O2—H2	0.72 (6)	C2—H2A	1.0000
O2—C3	1.313 (4)	C2—C3	1.519 (5)
O3—C3	1.211 (4)		
C2—O1—H1	109.5	O1—C2—H2A	108.6
C3—O2—H2	110 (5)	O1—C2—C3	109.2 (3)
I1—C1—H1A	109.3	C1—C2—H2A	108.6
I1—C1—H1B	109.3	C1—C2—C3	112.2 (3)
H1A—C1—H1B	108.0	C3—C2—H2A	108.6
C2—C1—I1	111.5 (2)	O2—C3—C2	112.6 (3)
C2—C1—H1A	109.3	O3—C3—O2	124.0 (3)
C2—C1—H1B	109.3	O3—C3—C2	123.4 (3)
O1—C2—C1	109.5 (3)		
I1—C1—C2—O1	59.5 (3)	O1—C2—C3—O3	6.6 (5)
I1—C1—C2—C3	−61.9 (3)	C1—C2—C3—O2	−52.8 (4)
O1—C2—C3—O2	−174.4 (3)	C1—C2—C3—O3	128.3 (4)

Hydrogen-bond geometry (Å, º)

D—H···*A*	*D*—H	H···*A*	*D*···*A*	*D*—H···*A*
O2—H2···O1^{i}	0.72 (6)	1.97 (6)	2.684 (4)	172 (7)
O2—H2···O3^{i}	0.72 (6)	2.68 (6)	3.101 (4)	120 (6)

Symmetry code: (i) *x*, −*y*+1/2, *z*−1/2.